Delft University of Technology

Direct submicron patterning of titanium for bone implants

Hammann, C.P.W.; Heerkens, C. Th H.; Hagen, C. W.; Zadpoor, A. A.; Fratila-Apachitei, L. E.

DOI
10.1016/j.mee.2018.03.018

Publication date
2018

Document Version
Final published version

Published in
Microelectronic Engineering

Citation (APA)
Hammann, C. P. W., Heerkens, C. T. H., Hagen, C. W., Zadpoor, A. A., & Fratila-Apachitei, L. E. (2018). Direct submicron patterning of titanium for bone implants. *Microelectronic Engineering*, *195*, 13-20. https://doi.org/10.1016/j.mee.2018.03.018

Important note
To cite this publication, please use the final published version (if applicable).
Please check the document version above.

Copyright
Other than for strictly personal use, it is not permitted to download, forward or distribute the text or part of it, without the consent of the author(s) and/or copyright holder(s), unless the work is under an open content license such as Creative Commons.

Takedown policy
Please contact us and provide details if you believe this document breaches copyrights.
We will remove access to the work immediately and investigate your claim.

This work is downloaded from Delft University of Technology.
For technical reasons the number of authors shown on this cover page is limited to a maximum of 10.

Green Open Access added to TU Delft Institutional Repository

'You share, we take care!' - Taverne project

https://www.openaccess.nl/en/you-share-we-take-care

Otherwise as indicated in the copyright section: the publisher is the copyright holder of this work and the author uses the Dutch legislation to make this work public.

Microelectronic Engineering 195 (2018) 13–20

Contents lists available at ScienceDirect

Microelectronic Engineering

journal homepage: www.elsevier.com/locate/mee

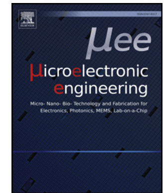

Research paper

Direct submicron patterning of titanium for bone implants

C.P.W. Hammann[a], C.Th.H. Heerkens[b], C.W. Hagen[b], A.A. Zadpoor[a], L.E. Fratila-Apachitei[a,*]

[a] Delft University of Technology, Faculty of Mechanical, Maritime and Materials Engineering, Department of Biomechanical Engineering, Delft 2628CD, The Netherlands
[b] Delft University of Technology, Faculty of Applied Sciences, Department of Imaging Physics, Delft 2628CJ, The Netherlands

ARTICLE INFO

Keywords:
Electron beam lithography
Reactive ion etching
Titanium
Direct patterning
Submicron
Bone implants

ABSTRACT

Recent research evidences the strong modulatory role of controlled submicron and nanoscale topographies on stem cells fate. To harness these physical surface cues for clinical applications, fabrication of nano- and submicron patterns on clinically relevant biomaterials is greatly needed. In this study, an electron beam lithography method for direct patterning (i.e., no use of masters/imprinting steps) of titanium in the submicron range was developed. The process required the use of an etch mask consisting of a double layer of SiO_2 and Al, and the positive AR P-6200.04 electron beam resist. An optimum electron beam dose of 288 μC/cm^2 was established for writing the desired patterns. The transfer of the patterns into the titanium substrates was achieved by three different steps: inductively coupled plasma etching of the mask in BCl_3/Cl_2 followed by reactive ion etching of titanium in $SF_6/CHF_3/O_2$ and a final wet etch of mask residue. Highly ordered arrays of titanium pits with submicron diameters were produced with high reproducibility. This method provides great versatility in pattern design, direct transfer into titanium and increased control of titanium pattern features at submicron to nanoscale enabling clinically relevant and systematic studies on pattern-induced cellular responses.

1. Introduction

Implants integration in the host tissues is largely determined by the early interactions taking place at the interface between biomaterial surface and relevant host cells. Recent research has evidenced the beneficial role of controlled submicron and nanoscale topographies for osteogenic differentiation of stem cells. The work of Dalby et al. [1] has shown that 120 nm diameter pits in poly(methyl methacrylate), having 100 nm depth, a centre-centre spacing of 300 nm and a controlled displacement of 50 nm from a square arrangement, could induce osteogenic differentiation of human mesenchymal stem cells in the absence of osteogenic supplements. By comparison, the patterns with an ordered square arrangement embossed in poly(caprolactone) and polycarbonate have retained their stem-cell phenotype [2,3]. Induced osteogenic differentiation was associated with changes in cells shape, focal adhesions size and cytoskeleton organization indicative of mediation by mechanotransduction pathways [4]. Patterns in the form of submicron pillars and pits produced on polystyrene surfaces by hot embossing (diameters of 200 nm, interspace of 500 nm) have been shown to stimulate osteogenic differentiation and mineralization of osteoblast-like cells, with more pronounced effects observed for the pits morphology [5]. The favorable *in vitro*effects of controlled submicron and nanoscale topographies on osteogenic differentiation are supported by recent *in vivo* studies [6,7]. Semispherical protrusions with a diameter of 79 ± 6 nm produced on titanium surfaces by colloidal lithography [6] suppressed early inflammatory events and enhanced osteogenic activity when inserted in rat tibia. In the other study [7], titanium surfaces with 15 nm high pillars produced by templated anodization resulted in about 20% increase of the bone-implant contact area relative to the polished surfaces following implantation for two months in rabbit femora. These findings indicate the strong potential of controlled topographical cues in the submicron to nanoscale for modulating cells response towards formation of new bone tissue with favorable effects on implants osseointegration.

In order to establish the cause-effect relationships between specific pattern features and cells response, and to achieve clinical benefits, such topographies should be generated on relevant biomaterials. In the case of bone implants, one of the most used biomaterials is titanium and its alloys. The method for surface modification should (i) have the required resolution to enable generation of submicron to nanoscale patterns, (ii) provide control of pattern features and versatility in shapes and spatial organization, (iii) be efficient for patterning sufficiently large areas for studies involving mammalian cells and (iv) ensure reproducibility. Most patterning methods used so far to create submicron/nanopatterns for studying osteogenic differentiation were developed for polymeric substrates and included a combination of processes such as optical lithography/nanoimprint [8], electron beam lithography (EBL)/nanoimprint [1,9–13] or templated anodization

* Corresponding author.
E-mail address: e.l.fratila-apachitei@tudelft.nl (L.E. Fratila-Apachitei).

https://doi.org/10.1016/j.mee.2018.03.018
Received 13 October 2017; Received in revised form 26 February 2018; Accepted 17 March 2018
Available online 19 March 2018
0167-9317/ © 2018 Elsevier B.V. All rights reserved.

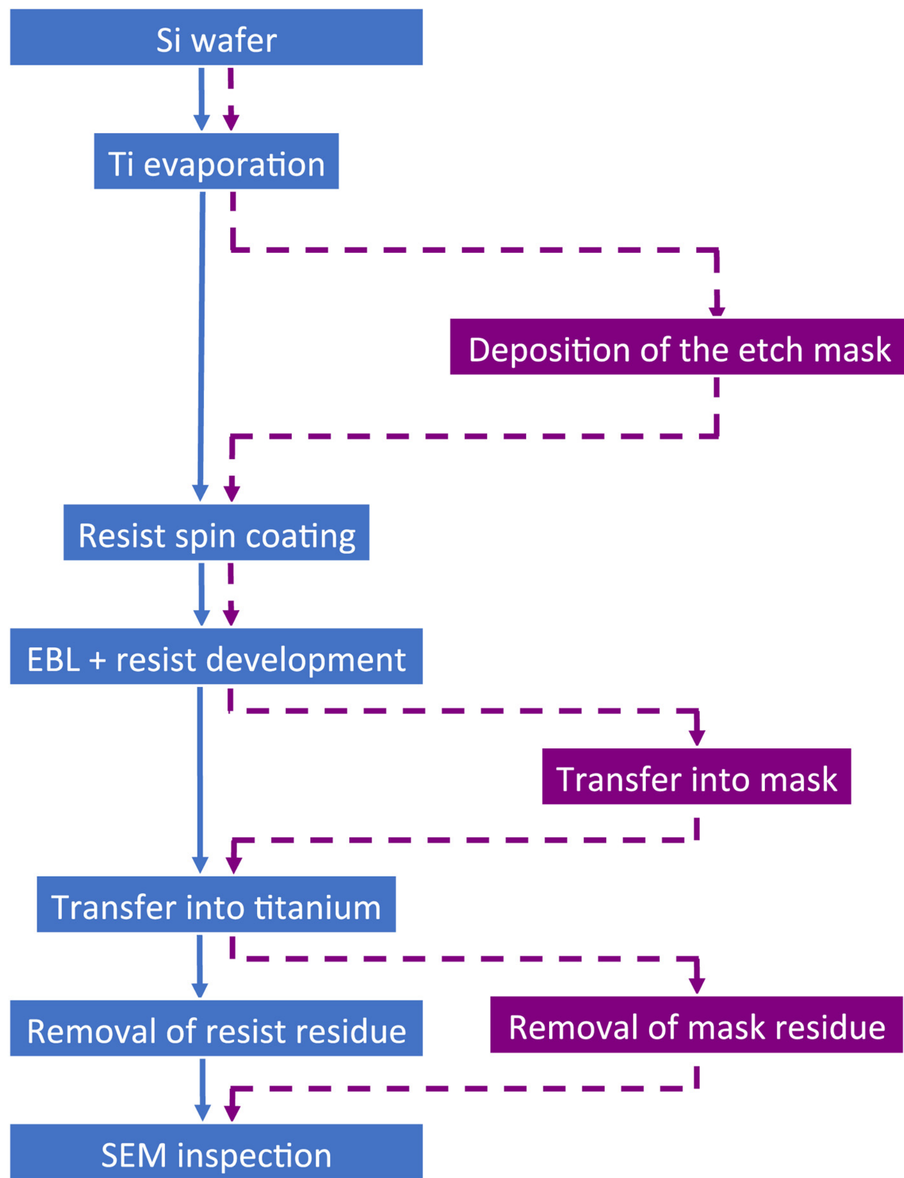

Fig. 1. Flowchart of the main processing steps used for the two routes investigated: without etch mask (continuous lines) and with etch mask (dotted lines).

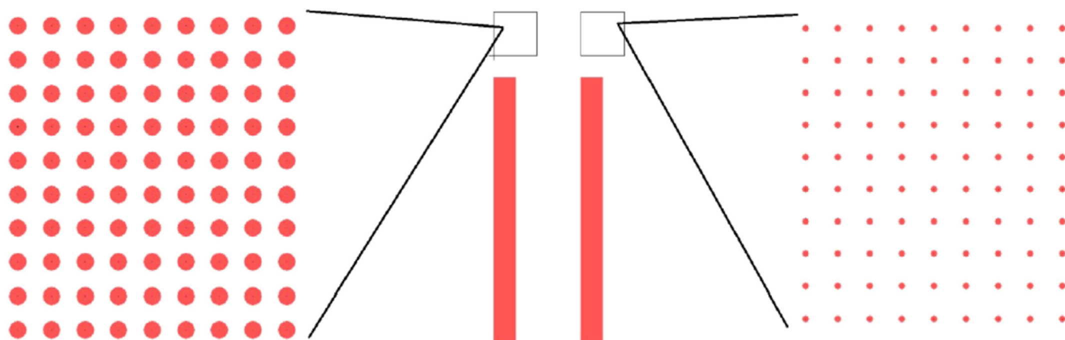

Fig. 2. Example of pattern design for EBL writing in the positive e-beam resist (500 nm and 100 nm diameters; 900 nm center-center distance; square arrangement).

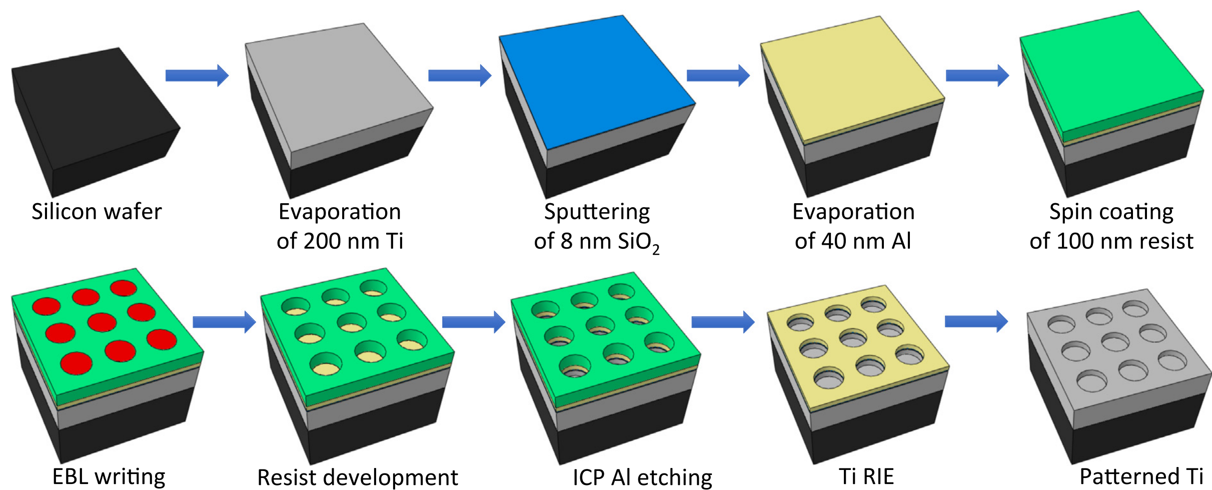

Fig. 3. Schematics of the EBL method for direct patterning of titanium (ICP = inductively coupled plasma; RIE = reactive ion etching).

[14,15] and colloidal lithography [6,16–18]. Among these methods, EBL has the potential to achieve the required resolution, the fine control and reproducibility of pattern features on titanium as well as the flexibility to design various shapes, sizes and spatial arrangements of the patterns.

However, most of the EBL methods developed so far for cells guidance have been used to actually create high resolution masters for subsequent patterning of polymeric substrates usually by replica molding and micro/nanoimprinting [1,9–13,19]. The need of a new master or mold for every different pattern and the difficulty to accurately imprint the patterns into metals [20,21] hinder the possibility to perform systematic research using various well-controlled patterns, and limit generation of a large number of different samples needed for such biological studies. A direct EBL method for Ti patterning would overcome these limitations and eliminate the use of additional imprinting steps.

Both, the type of substrate and pattern features determine the EBL processing steps and the materials and configuration needed for the resists and etch masks. Furthermore, the process requires experimental optimization of each step, from spinning of the resist to the transfer of the patterns into the substrate. Following-up the research on titanium-based microelectromechanical systems, a highly anisotropic dry etching process based on non-toxic fluorine chemistry has been recently developed for bulk titanium and used to produce square pillars in the micrometer range (5 × 5 × 5 μm) by EBL [22]. In the present study, the EBL process has been harnessed, to generate arrays of submicron pits directly in titanium surfaces.

2. Experimental

Two different fabrication routes were designed, namely without and with an etch mask (EM). The main process steps (Fig. 1) included evaporation of Ti on the Si wafer, deposition of the EM, spin coating of the electron beam resist, pattern writing in the resist by EBL, resist development and pattern transfer into the titanium substrate.

Firstly, a titanium layer of 200 ± 20 nm thickness was deposited by e-beam evaporation on a 525 μm thick 4-inch Si wafer (University Wafer, Inc.) using a TEMESCAL FC-2000 evaporation system. Titanium (99.5%) was evaporated at a rate of 2 Å/s and a pressure of 3×10^{-6} Torr. The resulting layer had an average surface roughness (R_a) of 3.8 nm as measured with a DektakXT stylus profilometer.

Secondly, the etch mask was deposited. The etch mask was adapted from [22]. It consisted of a SiO_2 layer of 8 ± 1 nm thickness, sputtered on the Ti substrate, and a 40 ± 4 nm Al layer evaporated on top of the SiO_2 layer.

Thirdly, the wafer was spin coated with e-beam resist. AR P-6200.04 (Allresist GmbH, Germany), based on poly(α-methyl styrene-*co*-α-chloroacrylate methyl ester) was used as a high resolution positive e-beam resist. A layer of 100 ± 10 nm thickness was applied by spin coating at 3500 rpm followed by a bakeout at 150 °C for 3 min.

The wafer was patterned by EBL at 100 keV using an EBPG-5000 + HR100 exposure tool (Raith GmbH). The beam current was 7.6 nA and the estimated spot size was 8–10 nm. Patterns design included dots with diameters of 50, 100 and 200 nm with a center-center spacing of 300 and 900 nm, and dots of 300 and 500 nm with 900 nm interspace in a square spatial arrangement (Fig. 2). A series of tests was performed to establish the optimum electron beam dose needed to produce the desired patterns in the resist. Ten different doses (200, 240, 288, 346, 415, 498, 597, 717, 860 and 1032 μC/cm^2) were applied to write patterns with various dot diameters, the relation between the dose and the feature area being given by Dose = (Beam current ∗ Dwell time) / (Feature area).

Following the development of the resist, the diameter of the patterns was determined from the scanning electron microscopy (SEM) images at 0° tilt angle by measuring the inner diameter of the opened patterns. The values obtained were compared with the designed diameter. The dose that resulted in patterns with the closest diameter to the intended values was established as optimum. The resist was developed by using three immersion steps: 60 s in amyl-acetate solution followed by 60 s in 1:1 methyl isobutyl ketone:isopropyl alcohol and another 60 s in isopropyl alcohol.

To transfer the patterns into the titanium substrate, using the route with the EM, the process included three different steps: etching of the mask, etching of the exposed titanium and removal of the remaining mask (Fig. 3). Aluminum was etched by using inductively coupled plasma (ICP) chlorine etching involving four different steps: (1) tempering at 50 °C, (2) breakthrough of the Al_2O_3 using BCl_3 (30 sccm) + Cl_2 (5 sccm) plasma for 25 s at 200 W, (3) Al and SiO_2 etching performed with the same plasma composition but a power of 100 W and a duration of 30 s and (4) the pump-out step. The etching equipment used was a PlasmaLab100 ICP Deep Reactive Ion Etcher (Oxford Instruments Plasma Technology). Titanium was etched by

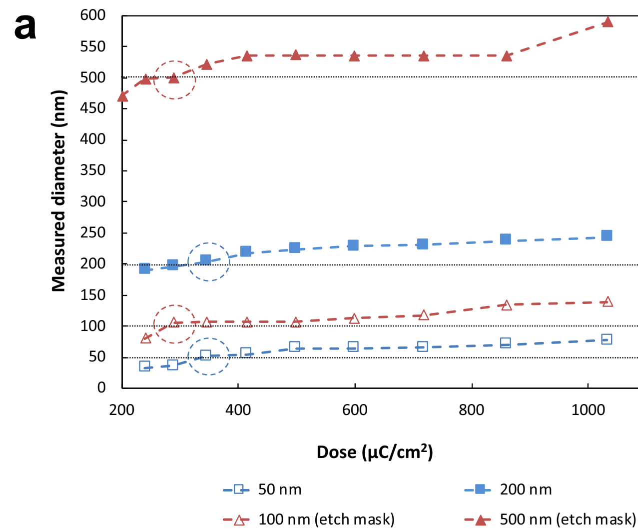

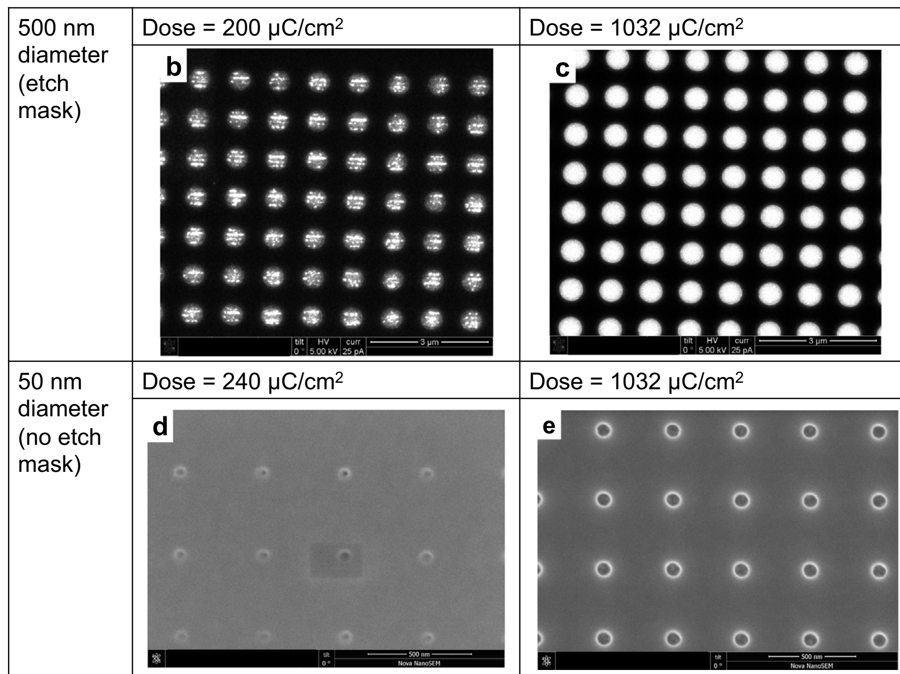

Fig. 4. (a) Effects of the applied dose on pattern diameters after development of the AR P-6200.04 resist (encircled values represent the optimum doses and the dotted horizontal lines represent the designed diameters); (b–e) examples of the patterns produced with low and high doses.

reactive ion etching (RIE) using a mixture of SF_6 (13 sccm) + CHF_3 (13 sccm) + O_2 (15 sccm) gases at 100 W for 180 s in a Leybold F system. Finally, the remaining mask was removed by wet etching using aluminum etch type D based on phosphoric acid, sodium-M-nitrobenzene sulfonate and acetic acid for 450 s (Transene Company, Inc.) and a buffered HF solution to remove the SiO_2.

For the route without the EM, pattern transfer involved RIE of Ti and removal of the residual resist by oxygen plasma using a Tepla stripper 100 equipment (PVA TePla AG) and an O_2 flow of 200 ml/min at 600 W for 10 min. Various recipes for Ti RIE have been tried including $50Cl_2 \pm 2.5Ar$ (1000 W, 15 s) [23,24], $20CF_4 + 50Ar$ (32 W with 300 s and 600 s) [25] and $13SF_6 + 13CHF_3 + 15O_2$ (100 W and 180 s) [22].

The patterns produced in the resist and the ones transferred into the Ti substrate were inspected by SEM using a FEI Nova NanoLab 650 Dual Beam system (Thermo Fisher Scientific). Images with various magnifications at 0° and 45° tilt were acquired using an acceleration voltage of 5 kV for the patterns written on the resist and an acceleration voltage of 15 kV for the titanium patterns. Furthermore, the titanium patterns were also imaged by atomic force microscopy (AFM) using a Fastscan AFM (Bruker) with a fastscan A tip at 0.502 Hz. 2D, 3D images as well as line profiles were acquired and used for quantification of the pit diameters (by measuring the openings at the same height selected just below the surface spikes, as indicated by the horizontal dashed lines in Fig. 7).

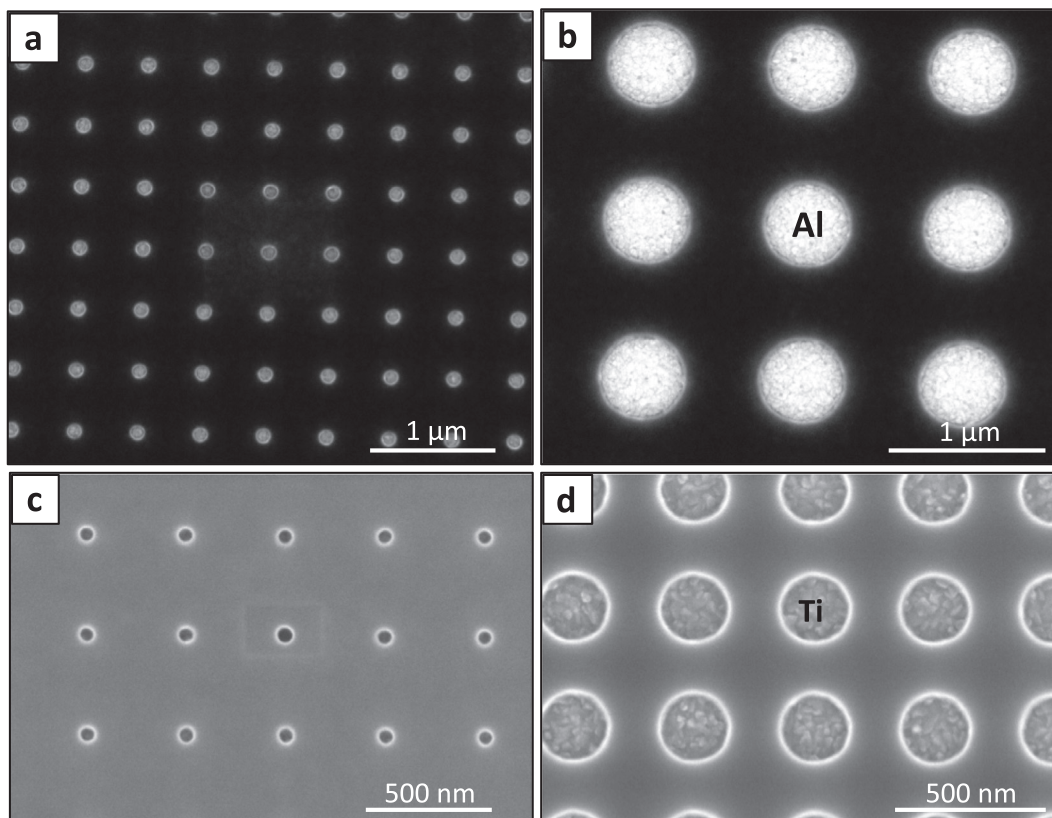

Fig. 5. Scanning electron micrographs of the patterns produced with the optimum dose: (a, b) 100 nm and 500 nm patterns (with etch mask); (c, d) 50 nm and 200 nm patterns (without the etch mask).

3. Results and discussion

3.1. Dose tests

The quantitative and qualitative effects of the ten different exposure doses on pattern features after resist development are presented in Figs. 4 and 5. During detailed inspection by SEM imaging at various magnifications it was observed that at the lowest doses (200 and 240 µC/cm^2), some patterns were not yet fully opened and the diameters of the open ones tended to be smaller than the designed value. For example, in the case of 500 nm patterns, the 200 µC/cm^2 dose did not fully open the patterns and the diameters measured from the SEM images were around 471 nm. In the case of 50 nm patterns, the 240 µC/cm^2 dose did not fully open the patterns and the diameter measured was only 30–40 nm. SEM images of these examples are included in Fig. 4(b–e). By increasing the dose, all patterns opened up fully and the diameters slowly increased. This trend was confirmed by the quantified data included in Fig. 4a. The patterns produced with the optimum dose with, respectively without the EM, are included in Fig. 5a and b, respectively c and d. The findings further indicated a different optimum dose for the two different routes investigated, i.e. 288 µC/cm^2 when the EM was used versus 346 µC/cm^2 when no EM was used. As the same resist type and thickness, acceleration voltage and developer were used, this difference may be related to the contribution of backscattering effects from the two different substrates (SiO_2/Al and Ti respectively) to the actual resist exposure dose. As the backscatter yield of Al is smaller than that of Ti at 100 keV (~0.133 for Al at 102 keV [26] and ~0.246 for Ti at 60 keV [27]) one would expect that a slightly higher dose is required when using the EM. In fact, the opposite is observed, the cause of which is not entirely clear. Perhaps the charging of the insulated Al layer may play a role here.

3.2. Transfer of the patterns into titanium

Without the EM, no patterns were visible after Ti RIE using the methods described in the experimental section, as the resist was removed during the process. This indicated the need to have an etch mask. Due to its inertness to fluorine, aluminum was considered as the etch mask. To enhance the adhesion of the Al layer to Ti and further stabilize the thin aluminum mask during Ti RIE, a layer of SiO_2 was sputtered on the Ti prior to Al evaporation (Fig. 3) [22].

The patterns were successfully transferred through the etch mask into the titanium substrate by a sequence of three steps involving chlorine ICP etching of aluminum, Ti fluorine RIE (using the 13SF_6 + 13CHF_3 + 15O_2 gas mixture at 100 W and 180 s) and removal of the mask residue by wet etching. Representative SEM and AFM images of the resulting titanium patterns are included in Figs. 6 and 7. Pits with diameters of 318 ± 25 nm and 732 ± 16 nm (based on AFM cross-section measurements, Fig. 7) have been produced with high reproducibility. Nevertheless, the diameters of the pits were larger than the designed diameters (100 nm and 500 nm, respectively) indicating isotropic etching. Note that in the line profiles of Fig. 7 the diameter of the pits is considerably smaller at the bottom of the pits, although this may be partly due to the convolution with the AFM tip diameter. During the RIE process used, titanium reacts with SF_6 and forms the volatile TiF_4 compound. CHF_3 is mostly responsible to control

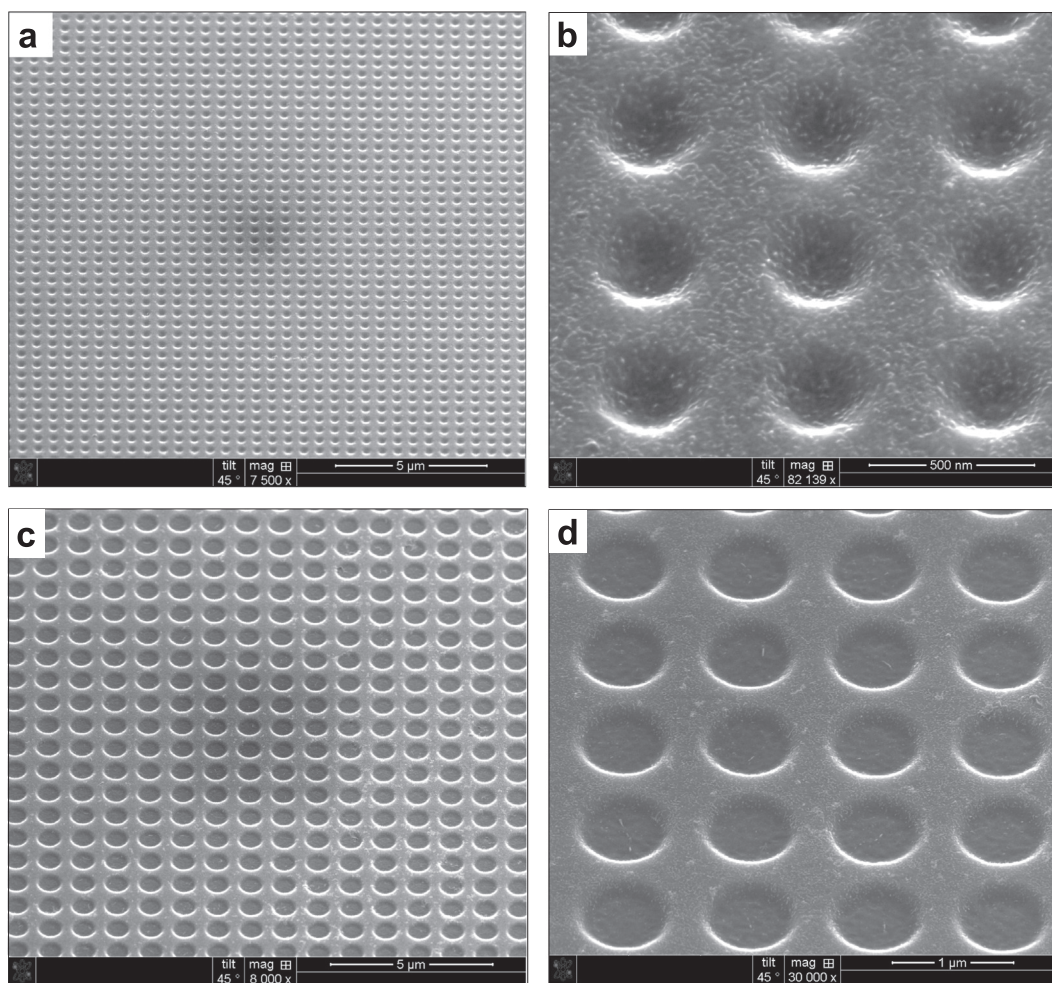

Fig. 6. Scanning electron micrographs of the titanium patterns (tilt 45°) produced using the Al/SiO_2 etch mask and three different etching steps: a and b arrays of small pits with ca 300 nm diameter at two different magnifications; c and d arrays of large pits with ca 714 nm pits at two different magnifications.

anisotropy during etching as it forms a fluorocarbon polymer on the pits sidewalls which acts as a passivation layer thus reducing the vertical etch rate. By optimizing the CHF_3/O_2 ratio a balance between anisotropy and acceptable etch rates may be achieved [22]. However, in the context of the application, before such an optimization is performed, the effects of anisotropy on cells response should be assessed.

One of the limitations of the proposed method is the time needed for e-beam writing of relatively large areas and for fabrication of a large number of samples needed for cell experiments. Under the used EBL conditions (exposure dose of 288 μC/cm^2 and a beam current of 7.6 nA) an area of 1 cm^2, filled with 732 nm patterns at a pitch of 1 μm, would take 4.4 h to write. Strategies to decrease the writing time include a reduction of the number of multiple exposures by increasing the spot size combined with the use of sensitive resists requiring lower doses [28]. Shorter times also benefit pattern quality due to less influence of stage drift. On the other side, the easiness to systematically change specific pattern features in the submicron and nanoscale with no masters needed, the accuracy to transfer these patterns into titanium without additional imprinting steps and the possibility to reuse the patterned samples (as compared to the polymeric ones) compensate for the time needed to generate such samples by EBL and guarantee high quality and reproducible biological results.

For the application of the EBL process on metallic bone implants such as total joint replacements, spinal cages or scaffolds, writing on 3D surfaces should be possible. New advances in the technology are needed such as the novel EBL systems with Z-lift stage able to write on curved surfaces. Another approach could be to make use of self-folding structures which enable access to the flat surface for patterning before folding to form the 3D structures. We have recently developed a platform for fabrication of 3D structures with free-form surface ornaments by combining self-foldable metallic structures with laser patterning and electron beam induced deposition [29]. Such materials provide a unique combination of properties and surface functionalities relevant for various applications including implants. Once the optimum pattern is established, EBL stamps in combination with imprinting can be used to increase scalability of such an approach.

Apart from generating topographical cues on various substrates, the EBL process can be used to control surface stiffness by e-beam radiation thereby inducing another cue known to modulate stem cells fate [30]. The process has been also applied for development of nano-channels used in biomolecular studies on DNA separation, sensing or stretching [31]. EBL is thus emerging as a method for fabrication of well-controlled submicron and nanoscale structures relevant for advanced biomedical research.

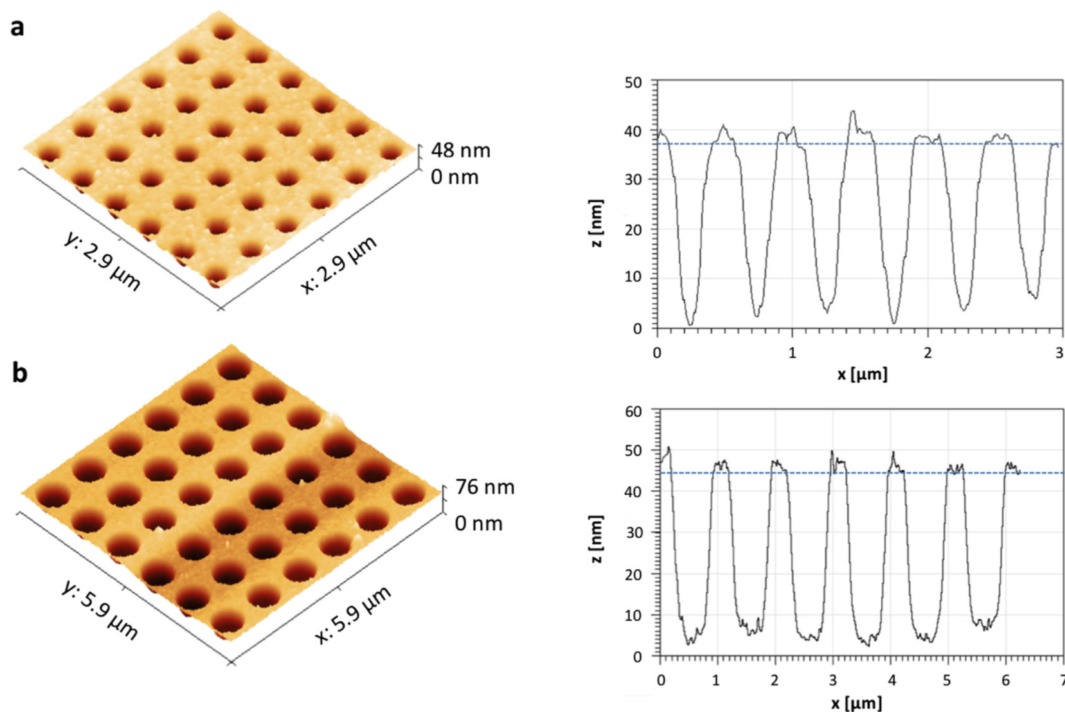

Fig. 7. 3D images and line profiles obtained by atomic force microscopy for the titanium patterns shown in Fig. 6. From the line profiles, the pit diameters were measured as: (a) 318 ± 25 nm; (b) 732 ± 16 nm.

4. Conclusions

In this study, an EBL method for the generation of submicron pits directly in titanium was developed, driven by the need to produce controlled submicron topography for modulating cellular responses at the interface between bone and titanium implants. The focus was on determining the optimum exposure dose and establishing the process steps for pattern transfer. An etch mask consisting of a double layer of Al and SiO_2 was required to produce the desired patterns. The presence of the etch mask affected the exposure dose and the subsequent steps for pattern transfer. An optimum dose of 288 $\mu C/cm^2$ was established for writing on the positive AR P-6200.04 electron beam resist. The patterns were successfully transferred into titanium by ICP chlorine etching of the mask, fluorine ($SF_6/CHF_3/O_2$) RIE of Ti and a final wet etching of the remaining mask. Following this method, arrays of submicron titanium pits were generated with high reproducibility. The versatility in pattern design and the direct transfer into titanium with superior control at submicron/nanoscale and no need for masters and imprinting steps make this method very attractive for systematic studies on pattern-induced cell fate, with impact on titanium clinical applications and future implant technology.

References

[1] M. Dalby, N. Gadegaard, R. Tare, A. Andar, M. Riehle, P. Herzyk, C. Wilkinson, R. Oreffo, The control of human mesenchymal cell differentiation using nanoscale symmetry and disorder, Nat. Mater. 6 (2007) 997–1003.
[2] R. McMurray, N. Gadegaard, P. Tsimbouri, K. Burgess, L. McNamara, R. Tare, K. Murawski, E. Kingham, R. Oreffo, M. Dalby, Nanoscale surfaces for the long-term maintenance of mesenchymal stem cell phenotype and multipotency, Nat. Mater. 10 (2011) 637–644.
[3] P.S. Tsimbouri, R.J. McMurray, K.V. Burgess, E.V. Alakpa, P.M. Reynolds, K. Murawski, E. Kingham, R.O.C. Oreffo, N. Gadegaard, M.J. Dalby, Using nanotopography and metabolomics to identify biochemical effectors of multipotency, ACS Nano (11) (2012) 10239–10249.
[4] S. Dobbenga, L.E. Fratila-Apachitei, A.A. Zadpoor, Nanopattern-induced osteogenic differentiation of stem cells – a systematic review, Acta Biomater. 46 (2016) 3–14.
[5] K.J. Cha, J.M. Hong, D.-W. Cho, D.S. Kim, Enhanced osteogenic fate and function of MC3T3-E1 cells on nanoengineered polystyrene surfaces with nanopillar and nanopore arrays, Biofabrication 5 (2013) 025007(12 pp.).
[6] D. Karazisis, A.M. Ballo, S. Petronos, H. Agheli, L. Emanuelsson, P. Thomsen, O. Omar, The role of well-defined nanotopography of titanium implants on osseointegration: cellular and molecular events in vivo, Int. J. Nanomedicine 11 (2016) 1367–1382.
[7] R.K. Silverwood, P.G. Fairhurst, T. Sjostrom, F. Welsh, Y. Sun, G. Li, B. Yu, P.S. Young, R.M.D. Meek, M.J. Dalby, P.M. Tsimbouri, Analysis of osteoclastogenesis/osteoblastogenesis on nanotopographical titania surfaces, Adv. Healthc. Mater. 5 (2016) 947–955.
[8] J. Kim, W. Bae, K. Lim, K. Jang, S. Oh, K. Jang, N. Jeon, K. Suh, J. Chung, Density of nanopatterned surfaces for designing bone tissue engineering scaffolds, Mater. Lett. 130 (2014) 227–231.
[9] A. Hart, N. Gadegaard, C. Wilkinson, R. Oreffo, M. Dalby, Osteoprogenitor response to low-adhesion nanotopographies originally fabricated by electron beam lithography, J. Mater. Sci. Mater. Med. 18 (2007) 1211–1218.
[10] M. Dalby, N. Gadegaard, M. Riehle, C. Wilkinson, A. Curtis, Investigating filopodia sensing using arrays of defined nano-pits down to 35 nm diameter in size, Int. J. Biochem. Cell Biol. 36 (2004) 2005–2015.
[11] N. Gadegaard, M. Dalby, M. Riehle, C. Wilkinson, Optimizing substrate disorder for bone tissue engineering of mesenchymal stem cells, J. Vac. Sci. Technol. B 26 (2008) 2554–2557.
[12] J.R. Wang, S.F. Ahmed, N. Gadegaard, R.M.D. Meek, M.J. Dalby, S.J. Yarwood, Nanotopology potentiates growth hormone signalling and osteogenesis of mesenchymal stem cells, Growth Hormon. IGF Res. 24 (2014) 245–250.
[13] A. Klymov, E. Bronkhorst, J.T. Riet, J. Jansen, X. Walboomers, Bone marrow-derived mesenchymal cells feature selective migration behavior on submicro- and nano-dimensional multi-patterned substrates, Acta Biomater. 16 (2014) 117–125.
[14] T. Sjöström, M. Dalby, A. Hart, R. Tare, R. Oreffo, B. Su, Fabrication of pillar-like tatania nanostructures on titanium and their interactions with human skeletal stem cells, Acta Biomater. 5 (2009) 1433–1441.
[15] L. McNamara, T. Sjöström, K. Burgess, J. Kim, E. Liu, S. Gordonov, P. Moghe, R. Meek, R. Oreffo, B. Su, M. Dalby, Skeletal stem cell physiology on functionally distinct titania nanotopographies, Biomaterials 32 (2011) 7403–7410.
[16] M. Dalby, D. McCloy, M. Robertson, H. Agheli, D. Sutherland, S. Affrossman, R. Oreffo, Osteoprogenitor response to semi-ordered and random nanotopographies, Biomaterials 27 (2006) 2980–2987.
[17] C. Berry, A. Curtis, R. Oreffo, H. Agheli, D. Sutherland, Human fibroblast and human bone marrow cell response to lithographically nanopatterned adhesive domains on protein rejecting substrates, IEEE Trans. Nanobioscience 6 (2007) 201–209.
[18] J. Fiedler, B. Özdemir, J. Bartholomä, A. Plettl, R. Brenner, The effect of substrate surface nanotopography on the behavior of multipotent mesenchymal stromal cells and osteoblasts, Biomaterials 34 (2013) 8851–8859.
[19] A. Connell, P.M. Reynolds, A. Saeed, N. Gadegaard, Fabrication of mesoscale topographical gradients in bulk titanium and their use in injection moulding, Microelectron. Eng. 164 (2016) 36–42.
[20] A. Greer, K. Seunarine, A. Khokhar, X. Li, D. Moran, N. Gadegaard, Direct nanopatterning of commercially pure titanium with ultra-nanocrystalline diamond stamps, Phys. Status Solidi A (9) (2012) 1721–1725.

[21] A. Greer, K. Seunarine, A. Khokhar, I. MacLaren, A. Brydone, D. Moran, N. Gadegaard, Increased efficiency of direct nanoimprinting on planar and curved bulk titanium through surface modification, Microelectron. Eng. 112 (2013) 67–73.
[22] R. Löffler, M. Fleischer, D.P. Kern, An anisotropic dry etch process with fluorine chemistry to create well-defined titanium surfaces for biomedical studies, Microelectron. Eng. 97 (2012) 361–364.
[23] E. Parker, B. Thibeault, M. Aimi, M. Rao, N. MacDonald, Inductively coupled plasma etching of bulk titanium, J. Electrochem. Soc. 10 (2005) C675–C683.
[24] O. Khandan, M. Kahook, M. Rao, Fenestrated microneedles for ocular drug delivery, Sensors Actuators B223 (2016) 15–23.
[25] I. Hotovy, I. Kostic, S. Hascik, V. Rehacek, M. Predanocy, A. Bencurova, Patterning of titanium oxide surface using inductively coupled plasma for gas sensing, Appl. Surf. Sci. 312 (2014) 107–111.
[26] H. Drescher, L. Reimer, M. Seidel, Backscattering and secondary electron emission of 10–100 keV electrons in scanning electron microscopy, Z. Phys. 29 (1970) 331–336.
[27] G. Neubert, S. Rogaschewski, Backscattering coefficient measurements of 15 to 60 keV electrons for solids at various angles of incidence, Phys. Status Solidi A 59 (1980) 35–41.
[28] N. Gadegaard, S. Thoms, D.S. Macintyre, K. Mcghee, J. Gallagher, B. Casey, C.D.W. Wilkinson, Arrays of nano-dots for cellular engineering, Microelectron. Eng. 67-68 (2003) 162–168.
[29] S. Janbaz, N. Noordzij, D.S. Widyaratih, C.W. Hagen, L.E. Fratila-Apachitei, A.A. Zadpoor, Origami lattices with free-form surface ornaments, Sci. Adv. 3 (2017) eaao1595.
[30] M. Lanniel, B. Lu, Y. Chen, S. Allen, L. Buttery, P. Williams, Patterning the mechanical properties of hydrogen silsesquioxane films using electron beam irradiation for application in mechano cell guidance, Thin Solid Films 519 (2011) 2003–2010.
[31] D. Xia, J. Yan, S. Hou, Fabrication of nanofluidic biochips with nanochannels for application in DNA analysis, Small 8 (2012) 2787–2801.